SUPPORTING INFORMATION

A 2.8 Å Fe–Fe Separation in the $Fe_2^{III/IV}$ Intermediate (X) from *Escherichia coli* Ribonucleotide Reductase

Laura M. K. Dassama,[1,2] Alexey Silakov,[1] Courtney M. Krest,[1] Julio C. Calixto,[1] Carsten Krebs,[1,2,*] J. Martin Bollinger, Jr.[1,2,*] and Michael T. Green[2,*]

Departments of [1]Chemistry and [2]Biochemistry and Molecular Biology, The Pennsylvania State University, University Park, Pennsylvania 16802, USA

EXPERIMENTAL PROCEDURES

Protein expression, purification and sample preparation. The methods for the overexpression and purification of *Ec* β-Y_{122}F have been described.[1,2] Two sets of samples containing the $Fe_2^{III/IV}$ complex (**X**) were prepared using the *in situ* generation of O_2 from ClO_2^-,[3] but with the substitution of *iso*-pentane with liquefied ethane (T ~ -150 °C) as the cryo-solvent. After evaporation of ethane at ~ -130 °C under reduced pressure, the powdered samples were packed into Mössbauer and EXAFS sample holders that have been described.[4] The final concentrations of components for the first set of samples (batch **1**) were 4.26 mM β, 6.19 mM ^{57}Fe, 10 mM ascorbate, 20 μM Cld, and 16 mM ClO_2^-. The second set of samples (batch **2**) contained 4.26 mM β, 6.16 mM Fe, 20 μM Cld, and 16 mM ClO_2^-. All reactions to generate **X** were quenched 0.3 s after mixing the reaction components at 5 °C.

To prepare samples containing reactant $Fe_2^{II/II}$ (diferrous) complex, a 3 mL solution of O_2-free β (4.26 mM), $^{57}Fe^{II}$ (6.16 mM), and Cld (20 μM) was sprayed into liquefied ethane in a rapid freeze-quench setup. Upon removal of the cryo-solvent, the frozen powdered sample was packed into Mössbauer and EXAFS sample holders as previously described.[4]

Samples containing the μ-oxo-$Fe_2^{III/III}$ (diferric) product complex were initially prepared and quenched in a manner identical to samples containing **X** (batch **2**). Upon removal of the liquefied ethane, the frozen powdered sample was allowed to thaw at ~ 5 °C for 1 hr before being re-loaded into the freeze-quench syringe and again sprayed into liquefied ethane. The cryo-solvent was removed and the powdered sample packed into Mössbauer and EXAFS samples holders, as previously described.[4] The final concentrations of components were identical to those present in the samples of **X** (batch **2)**.

^{57}Fe-Mössbauer spectroscopy. The Mössbauer spectrometer has been described.[5] Spectra were collected at 4.2 K with a 53-mT magnetic field externally applied either parallel or perpendicular to the γ-beam. The relative amount of intermediate **X** contained in the samples was estimated by analysis of the Mössbauer spectra using the program WMOSS (Seeco, Edina, MN). For the spectral deconvolution, we used experimental reference spectra of the reactant $Fe_2^{II/II}$ and the μ-oxo-$Fe_2^{III/III}$ product complexes (Figure **S3**), while the features of intermediate **X** were simulated using the commonly used spin Hamiltonian formalism[6] with parameters reported previously.[7] The relative amount of **X** can also be obtained from analysis of the difference spectrum (parallel – perpendicular), because only the spectral features of **X** depend on the orientation of the magnetic field.

XAS Data Collection and Analysis. All data were acquired in fluorescence mode at low temperature (~ 10 K) with a 30-element germanium detector (SSRL, BL7-3) as previously described.[4] A Si(220) ϕ = 0 monochromator with a 9.5 keV cutoff for harmonic rejection was used. Each scan was acquired for 35 mins. Data acquired on a portion of the sample previously unexposed to X-rays are referred to as first-scans. The background from the data was removed using the program EXAFSPAK (k-weight = 3; spline range k = 0.3 – 16 $Å^{-1}$). EXAFS data were analyzed using EXAFSPAK (available

at http://www-ssrl.slac.stanford.edu/exafspak.html), using ab initio phases and amplitudes generated by the program FEFF v7.0,[8,9] as previously described.[4] Distances and Debye-Waller factors (except for those contributed by the fraction of the diferric product in the data of the samples containing **X**) were treated as adjustable parameters.

The XAS data from the two preparations of **X** were analyzed individually before being combined to yield higher quality data. Only first scans were used for the analysis presented in the main manuscript. A total of eighty-three first scans were averaged for the analysis of the data acquired for samples of **X**. Second-scans were acquired to assess the extent of photoreduction or radiative damage.

Density Functional Theory Calculations. All DFT calculations have been performed using Gaussian 03 package.[10] Geometry optimizations were performed on the modified coordinates from X-ray crystal structure of *Ec* RNR-β (PDB: 1RIB).[11] First, a rough optimization was carried out for the high spin (HS) state i.e. assuming ferromagnetic coupling between iron centers, using spin-unrestricted BP86[12,13] DFT method *in vacuo* with Aldrichs SVP basis set on all atoms.[14] During the optimization the linking H atoms on all the ligating amino acids were fixed. Using obtained geometries, a broken symmetry state (BS) determinant emulating the antiferromagnetic coupling with S_{tot}=1/2 have been formed by permutating the HS wavefunctions so that in the α-spin domain only the d-orbitals of Fe^{III} (S=5/2) are populated and only the d-orbitals of Fe^{IV} (S=2) are populated in the β-spin domain.[15] Permutations were defined using home written programs based on the largest contributions to the wavefunctions. The obtained solutions were projected to a larger basis set 6-31G*, re-converged with a single-point calculation on the unrestricted B3LYP[16,17] level *in vacuo* and tested for stability.

A second step of the geometry optimization was carried out using a larger basis sets (Fe: 6-311G*, other atoms 6-31G) utilizing the obtained BS wavefunctions as initial guess. In this case a Gaussian implementation of the solvation model COSMO[18] (C-PCM)[19] has been utilized to account for the protein environment. Similar to the initial step the linking H atoms on all the ligating amino acids were fixed.

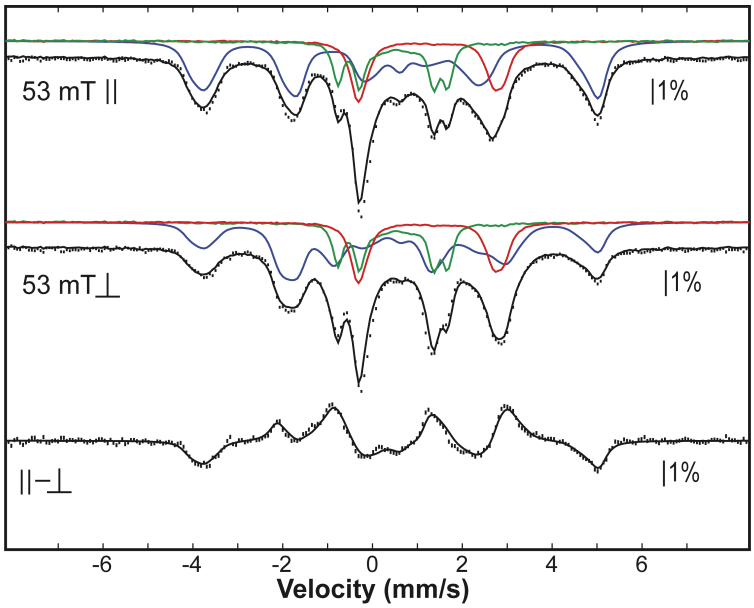

Figure S1. 4.2-K Mössbauer spectra of samples (**X**, batch **1**) used for XAS. Spectra were collected with a 53-mT magnetic field applied parallel (top) or perpendicular (middle) to the γ-beam. The vertical bars depict the experimental data, whereas the solid black lines represent the sum of the individual components. The red and green lines are the experimental reference spectra of the $Fe_2^{II/II}$ reactant and μ-oxo-$Fe_2^{III/III}$ product complexes (Figure **S3**), scaled to 20% and 22%, respectively. The blue lines are simulations of **X** using the published parameters,[7] scaled to 62% of the total area. The experimental difference spectrum (vertical bars, bottom) only depends on the features of **X**, because the features of the $Fe_2^{II/II}$ and μ-oxo-$Fe_2^{III/III}$ forms do not depend on the orientation of the magnetic field and therefore cancel out, and therefore provide an alternative way to determine the amount of **X** from the amplitude of the difference spectrum. The solid black line overlaid with the difference spectrum is the simulation of **X**, assuming 62% intensity.

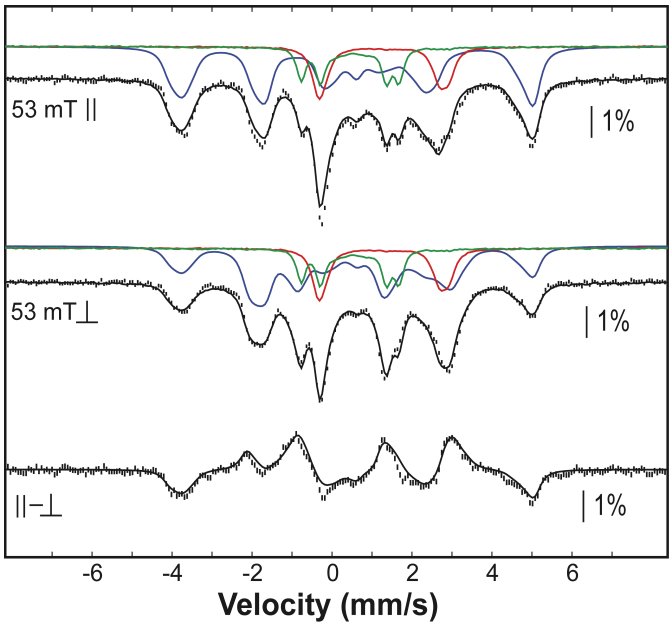

Figure S2. 4.2-K/53-mT Mössbauer spectra of samples containing **X** (batch **2**) used for XAS. The orientation of the 53-mT magnetic field is indicated at the left side of the spectra. Samples were analyzed as described in the legend of Figure **S1**. There is an 18% contribution to the spectra from the unreacted $Fe_2^{II/II}$ complex (red), and an 18% contribution from the μ-oxo-$Fe_2^{III/III}$ product complex. The contribution of **X** (blue) is scaled to 67% of the total intensity.

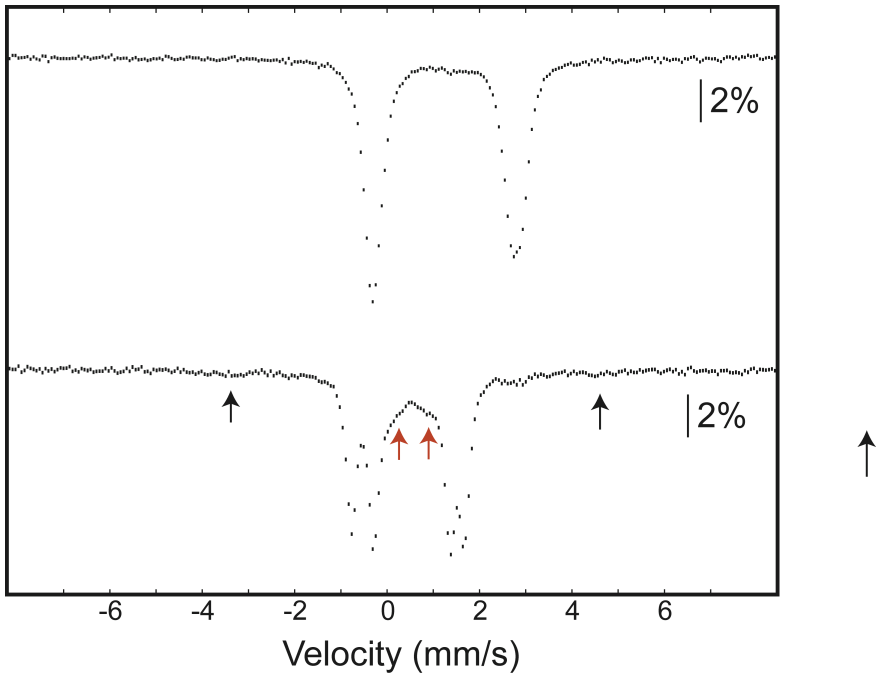

Figure S3. 4.2-K/53-mT Mössbauer spectra of samples containing the reactant $Fe_2^{II/II}$ complex (top) and the μ-oxo-$Fe_2^{III/III}$ product complex (bottom) of *Ec* β-$Y_{122}F$ used for XAS. The samples were prepared as described (*vide supra*). The spectrum of the reactant complex is a broad quadrupole doublet with parameters typical of high-spin Fe^{II}. The spectrum of the product complex exhibits the prominent features of the μ-oxo-$Fe_2^{III/III}$ complex in addition to minor amounts of a magnetically split feature on the baseline (tentatively attributed to a high-spin Fe^{III} contaminant; ~ 10%, see black arrows) and a weak absorption in the central portion of the spectrum (tentatively assigned to a non-μ-oxo-$Fe_2^{III/III}$ form; < 5%, see red arrows).

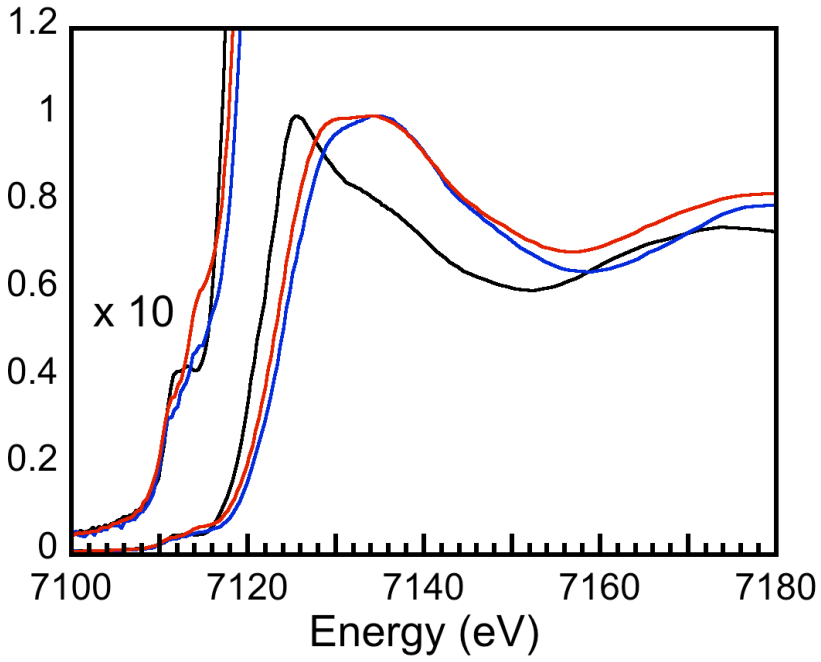

Figure S4. X-ray Absorption Near Edge Structure (XANES) spectra of samples containing **X** (red), the $Fe_2^{II/II}$ reactant complex (black), and the μ-oxo-$Fe_2^{III/III}$ product state (blue). The edge of the samples containing **X** is at a higher energy than the edge of samples containing the reactant complex, but appears at energy *lower* than that of the samples containing the product state. The presence of an unreacted $Fe_2^{II/II}$ component in the samples containing **X** may skew the edge toward a lower energy. Alternatively, this skewing of the edge toward a lower energy is a feature of **X** that remains to be understood.

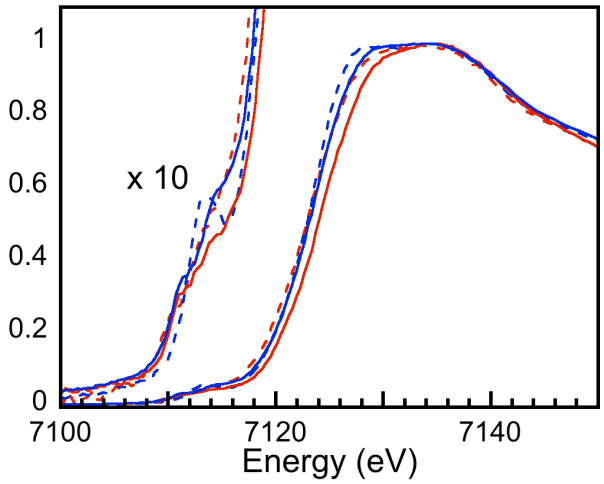

Figure S5. XANES spectra of samples containing **X** (blue), and the μ-oxo-$Fe_2^{III/III}$ a product complex sample (red). The spectra depicted in the solid lines arise from the first-scans, and the ones depicted in dashed lines are from the second-scans of the same portion of the samples. The edge energy in the spectra of the second-scans of the product complex shifts to a lower value while that of **X** does not change.

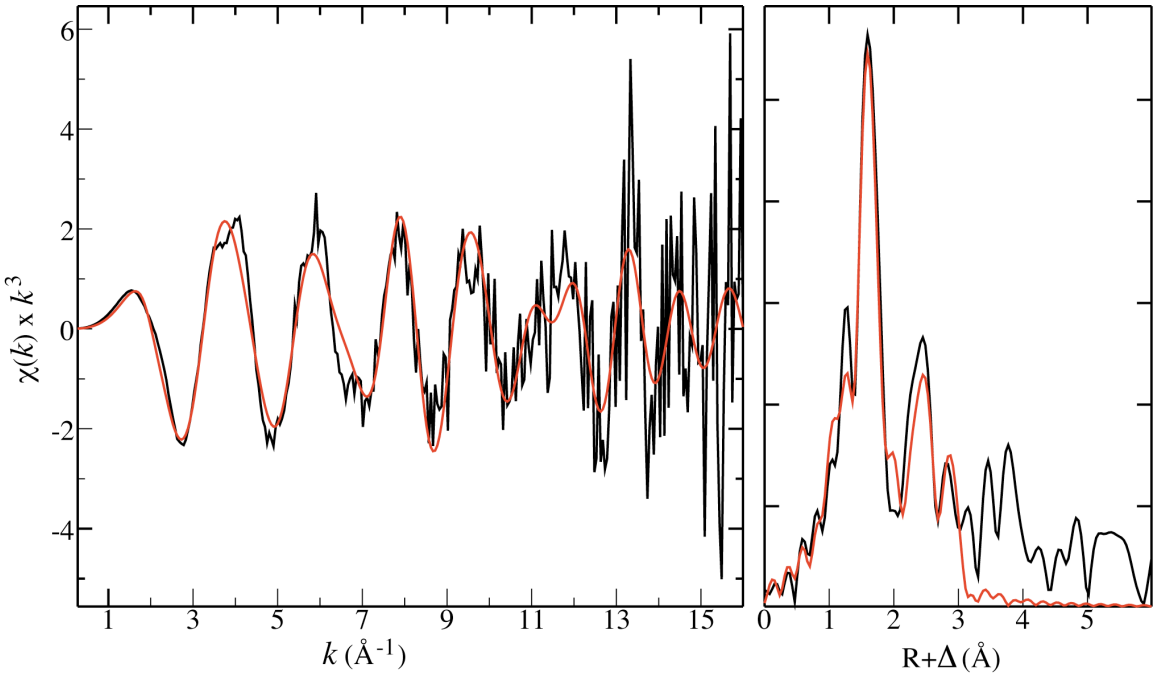

Figure S6. Second-scan EXAFS data (left) and its FT (right) of samples containing **X**. The prominent Fe-Fe scattering interaction at 2.8 Å in the EXAFS data from the first-scan data is still present. Fitting results are provided in Table **S8**.

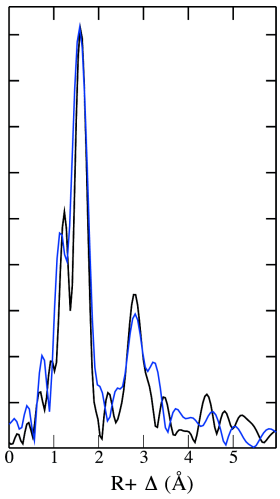

Figure S7. FT of EXAFS data evaluated at two extreme ranges of *k* for samples containing the μ-oxo-$Fe_2^{III/III}$ product complex. The black spectrum depicts the FT of the EXAFS data plotted over $k = 0.3 - 14$ Å^{-1}, whereas the blue spectrum depicts the same data plotted over $k = 0.3 - 11$ Å^{-1}.

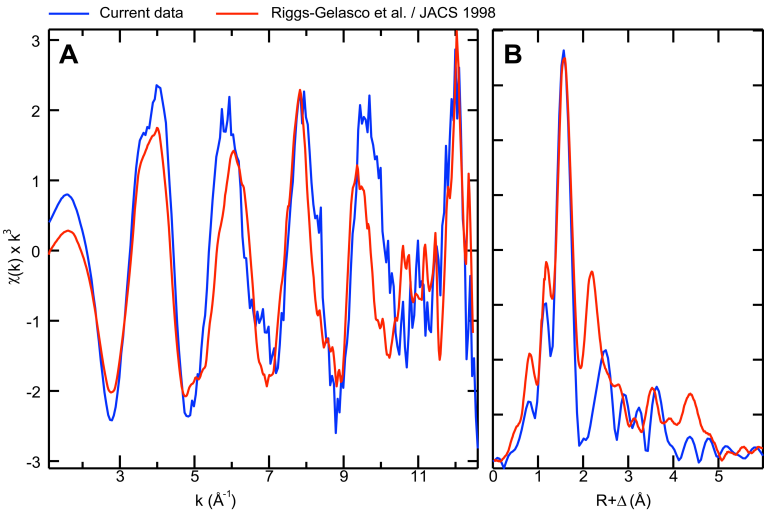

Figures S8. EXAFS data (**A**) and resulting FTs (**B**) of samples containing **X** reported by Riggs-Gelasco et al.[20] (red) and reported herein (blue).

Table S1. Additional EXAFS fitting (k = 0.3 – 14 Å^{-1}) results of samples containing the $Fe_2^{II/II}$ reactant complex used for XAS.

		Fe-O/N			Fe-O/N			Fe-O/N					
N_{tot}	S_0	N	R	σ^2	N	R	σ^2	N	R	σ^2	E_0	F	Res.
3	0.9	3	2.05	0.00459	0	-	-	0	-	-	-16.705	0.5601	0.114
		2	2.04	-0.0006	1	2.16	-0.0018	0	-	-	-11.799	0.4652	
		0	**-**	**-**	**3**	**2.03**	**0.00529**	**0**	**-**	**-**	**-16.05**	**0.4972**	
		1	2.01	-0.0021	2	2.11	0.00128	0	-	-	-11.803	0.4382	
		1	2.19	-0.0010	1	2.07	0.00044	1	2.01	-0.0005	-11.388	0.4107	
		0	-	-	2	2.12	0.00196	1	2.00	-0.0014	-10.873	0.4150	
4	0.9	4	2.05	0.00614	0	-	-	0	-	-	-16.787	0.5116	0.114
		3	2.06	0.00137	1	2.18	-0.0014	0	-	-	-11.597	0.4129	
		2	2.03	-0.0001	2	2.14	0.00128	0	-	-	-11.835	0.4035	
		2	2.16	0.00386	1	2.00	-0.0008	1	2.09	0.00318	-10.325	0.3782	
		1	2.21	-0.0007	3	2.04	0.0039	0	-	-	-11.697	0.3665	
		1	2.10	0.00769	2	2.03	0.00117	1	2.18	-0.0003	-11.235	0.3777	
		0	-	-	3	2.04	0.00273	1	2.19	-0.0004	-11.462	0.3739	
		0	**-**	**-**	**2**	**2.02**	**0.0086**	**2**	**2.15**	**0.00212**	**-10.986**	**0.3761**	
		0	-	-	4	2.04	0.00712	0	-	-	-15.296	0.4591	
5	0.9	5	2.06	0.00773	0	-	-	0	-	-	-15.775	0.4830	0.114
		4	2.14	0.00625	1	2.00	-0.0003	0	-	-	-10.337	0.3688	
		3	2.17	0.00411	2	2.02	0.00148	0	-	-	-10.659	0.3639	
		3	2.10	0.00972	1	2.01	-0.0007	1	2.15	0.00131	-11.224	0.3706	
		2	**2.20**	**0.00217**	**3**	**2.03**	**0.00308**	**0**	**-**	**-**	**-11.326**	**0.3631**	
		2	2.19	0.00114	2	2.04	0.0094	1	1.97	0.00613	-12.351	0.3592	
		1	2.22	-0.0001	4	2.04	0.005	0	-	-	-12.188	0.3670	
		1	2.21	-0.0006	3	2.04	0.003	1	1.97	0.01845	-13.324	0.3593	
		1	1.99	0.01395	2	2.15	0.00212	2	2.02	0.00088	-12.581	0.3690	
		0	-	-	5	2.04	0.00896	0	-	-	-15.091	0.4492	
		0	-	-	4	2.05	0.00481	1	2.21	0.00024	-11.794	0.3756	
		0	-	-	3	2.03	0.00295	2	2.17	0.00288	-11.606	0.3769	
6	0.9	6	2.07	0.00921	0	-	-	0	-	-	-15.249	0.4727	0.114
		5	2.07	0.00491	1	2.21	-0.0002	0	-	-	-12.231	0.3938	
		4	2.05	0.00313	2	2.18	0.00212	0	-	-	-12.054	0.4019	
		4	1.99	0.00450	1	2.18	-0.0043	1	2.06	-0.0042	-17.051	0.4392	
		3	2.03	0.00230	3	2.15	0.00448	0	-	-	-11.941	0.4006	
		3	2.03	0.01610	2	2.13	0.00295	1	2.00	-0.0009	-13.551	0.3709	
		2	2.02	0.00168	4	2.12	0.00706	0	-	-	-11.639	0.3974	
		2	1.96	0.00246	3	2.13	0.00193	1	2.02	-0.0025	-14.262	0.3857	
		2	1.98	0.01945	2	2.15	0.00022	2	2.02	0.0009	-13.766	0.3684	
		1	2.02	0.00022	5	2.10	0.00981	0	-	-	-11.535	0.3936	
		1	1.90	0.00936	4	2.10	0.00659	1	1.99	-0.0003	-13.493	0.3700	
		1	**1.88**	**0.00735**	**3**	**2.12**	**0.00398**	**2**	**2.00**	**0.00084**	**-14.368**	**0.3684**	
		0	-	-	6	2.04	0.01073	0	-	-	-14.862	0.4584	
		0	-	-	5	2.05	0.00676	1	2.22	0.00099	-12.435	0.4015	
		0	-	-	4	2.03	0.00482	2	2.19	0.00366	-11.640	0.4016	
		0	-	-	3	2.02	0.00360	3	2.16	0.00593	-11.383	0.4007	
4.5	**0.9**	**0**	**-**	**-**	**2**	**2.01**	**0.00126**	**2.5**	**2.15**	**0.00366**	**-10.969**	**0.3733**	**0.114**

N: coordination number or occupancy; **R**: distance (Å); **σ^2**: Debye-Waller factor (Å^2); **E_0**: threshold energy shift (eV); **F**: fit error defined as $(\Sigma k^6(\chi_{exptl} - \chi_{calc})^2/\Sigma k^6 \chi_{exptl}^2)^{1/2}$; Res: Resolution (Å). Unusually high and negative Debye-Waller factors are shown in blue and red, respectively. The best fits for each coordination number are shown in bold. Fit reported in the main manuscript is shown in green.

Table S2. Additional EXAFS (k=0.3-14 Å^{-1}) fitting results of samples containing the $Fe_2^{III/III}$ product complex used for XAS.

		Fe-O/N			Fe-O/N			Fe-O/N			Fe-Fe					
N_{tot}	S_0	N	R	σ^2	N	R	σ^2	N	R	σ^2	N	R	σ^2	E_0	F	Res.
3	0.9	3	2.05	0.00328	0	-	-	0	-	-	1	3.22	0.00428	-7.3744	0.5296	0.113
		2	2.13	0.00179	1	2.00	-0.0017	0	-	-	1	3.24	0.00485	-3.1842	0.4799	
		0	**-**	**-**	**3**	**2.03**	**0.0041**	**0**	**-**	**-**	**1**	**3.23**	**0.00461**	**-6.5815**	**0.5003**	
		1	2.18	-0.0007	2	2.03	0.0002	0	-	-	1	3.24	0.00514	-3.6001	0.4714	
		1	2.02	0.00464	1	2.02	-0.0025	1	2.14	-0.0016	1	3.24	0.00490	-4.6035	0.4705	
		0	-	-	2	2.02	0.00015	1	2.15	-0.0003	1	3.24	0.00485	-3.9878	0.4737	
4	0.9	4	2.05	0.00501	0	-	-	0	-	-	1	3.22	0.00421	-7.0203	0.5037	0.113
		3	2.12	0.00403	1	2.01	-0.0015	0	-	-	1	3.24	0.00476	-3.545	0.4603	
		2	2.16	0.00130	2	2.03	-0.0004	0	-	-	1	3.24	0.00482	-3.5520	0.4604	
		2	1.88	0.00810	1	1.98	-0.0050	1	2.10	-0.0050	1	3.19	0.00379	-15.849	0.5320	
		1	2.19	-0.0010	3	2.05	0.00116	0	-	-	1	3.24	0.00472	-4.1951	0.4594	
		1	2.17	-0.0018	2	2.03	-0.0006	1	1.90	0.00654	1	3.23	0.00502	-7.0569	0.4361	
		0	**-**	**-**	**3**	**2.03**	**0.00260**	**1**	**2.19**	**0.00144**	**1**	**3.24**	**0.00496**	**-4.0207**	**0.4642**	
		0	-	-	2	2.02	0.00132	2	2.14	0.00475	1	3.24	0.00488	-3.8202	0.4647	
		0	-	-	4	2.04	0.00610	0	-	-	1	3.23	0.00451	-6.4505	0.4937	
5	0.9	5	2.06	0.00661	0	-	-	0	-	-	1	3.23	0.00419	-6.9249	0.5008	0.113
		4	2.06	0.00301	1	2.19	0.00073	0	-	-	1	3.24	0.00451	-4.7950	0.4648	
		3	2.04	0.00181	2	2.15	0.00369	0	-	-	1	3.23	0.00462	-4.4614	0.4644	
		3	2.03	0.0002	1	2.15	-0.0015	1	1.85	0.00830	1	3.22	0.00411	-8.2783	0.4462	
		2	2.03	0.00129	3	2.12	0.00743	0	-	-	1	3.24	0.00479	-3.9554	0.4643	
		2	2.01	-0.0011	2	2.10	0.00037	1	1.84	0.00653	1	3.22	0.00442	-8.4700	0.4313	
		1	**1.81**	**0.00351**	**4**	**2.08**	**0.00509**	**0**	**-**	**-**	**1**	**3.21**	**0.00446**	**-11.127**	**0.4422**	
		1	1.85	0.00246	3	2.01	0.00093	1	2.14	-0.0009	1	3.22	0.00464	-8.7869	0.4175	
		1	1.86	0.00267	2	1.99	-0.0004	2	2.11	0.00147	1	3.22	0.00469	-8.0726	0.4173	
		0	-	-	5	2.04	0.00808	0	-	-	1	3.22	0.00446	-6.6565	0.5087	
		0	-	-	4	2.04	0.00466	1	2.21	0.00237	1	3.23	0.00475	-4.6489	0.4735	
		0	-	-	3	2.03	0.00319	2	2.18	0.00691	1	3.24	0.00504	-3.5662	0.4720	
6	0.9	6	2.06	0.00819	0	-	-	0	-	-	1	3.22	0.00414	-7.1531	0.5281	0.113
		5	2.06	0.00479	1	2.22	0.00124	0	-	-	1	3.23	0.00445	-4.7736	0.4764	
		4	2.05	0.00362	2	2.18	0.00582	0	-	-	1	3.23	0.00451	-4.3857	0.4782	
		4	2.03	0.00187	1	2.15	-0.0006	1	1.81	0.00504	1	3.22	0.00410	-9.0952	0.4312	
		3	2.04	0.00308	3	2.14	0.01035	0	-	-	1	3.24	0.00465	-4.3280	0.4769	
		3	**2.01**	**0.00068**	**2**	**2.11**	**0.00126**	**1**	**1.81**	**0.00450**	**1**	**3.22**	**0.00432**	**-9.1042**	**0.4216**	
		2	2.04	0.00206	4	2.08	0.01807	0	-	-	1	3.23	0.00443	-5.9278	0.4711	
		2	1.99	0.00007	3	2.08	0.00287	1	1.80	0.00337	1	3.21	0.00450	-9.5880	0.4112	
		2	2.01	-0.0007	2	2.11	0.00104	2	1.87	0.01343	1	3.22	0.00435	-9.1531	0.4255	
		1	2.04	-0.0004	5	2.06	0.01562	0	-	-	1	3.23	0.00464	-6.0324	0.4632	
		1	1.97	-0.0008	4	2.05	0.00467	1	1.80	0.00264	1	3.21	0.00464	-9.7865	0.4073	
		1	1.99	-0.0020	3	2.08	0.00272	2	1.86	0.0105	1	3.22	0.00453	-9.5391	0.4140	
		0	-	-	6	2.04	0.01024	0	-	-	1	3.22	0.00440	-6.8608	0.5336	
		0	-	-	5	2.04	0.00675	1	2.25	0.00273	1	3.23	0.00484	-4.8427	0.4925	
		0	-	-	4	2.04	0.00509	2	2.22	0.00934	1	3.24	0.00479	-4.0042	0.4849	
		0	-	-	3	2.02	0.00365	3	1.87	0.02018	1	3.20	0.00432	-12.129	0.4513	
7	0.9	7	2.06	0.00993	0	-	-	0	-	-	1	3.23	0.00420	-7.2126	0.5332	0.113
		6	2.06	0.01922	1	2.03	-0.0001	0	-	-	1	3.23	0.00478	-6.9644	0.4500	
		5	2.05	0.00539	2	2.20	0.00844	0	-	-	1	3.23	0.00444	-5.0239	0.4959	
		5	2.03	0.00356	1	2.16	0.00050	1	1.79	0.00377	1	3.22	0.00418	-9.3557	0.4228	
		4	1.90	0.02175	3	2.02	0.00365	0	-	-	1	3.20	0.00432	-12.188	0.4456	
		4	2.01	0.00258	2	2.12	0.00257	1	1.79	0.00326	1	3.21	0.00422	-9.7070	0.4171	

3	2.04	0.00337	4	1.94	0.03097	0	-	-	1	3.22	0.00411	-10.584	0.4700
3	1.99	0.00205	3	2.09	0.00416	1	1.79	0.00299	1	3.21	0.00438	-9.6820	0.4104
3	2.02	0.00055	2	2.12	0.00127	2	1.83	0.01046	1	3.21	0.00416	-10.346	0.4249
2	2.05	0.00184	5	2.02	0.02613	0	-	-	1	3.22	0.00432	-8.4129	0.4691
2	1.98	0.00165	4	2.06	0.00556	1	1.77	0.00237	1	3.21	0.00446	-9.9947	0.4068
2	2.00	-0.0001	3	2.09	0.00299	2	1.83	0.00931	1	3.21	0.00437	-10.309	0.4146
1	2.04	-0.0005	6	2.05	0.01958	0	-	-	1	3.22	0.00459	-6.9413	0.4671
1	**1.98**	**0.00053**	**5**	**2.04**	**0.00754**	**1**	**1.79**	**0.00248**	**1**	**3.22**	**0.00453**	**-9.7318**	**0.4064**
1	1.99	-0.0012	4	2.06	0.00460	2	1.83	0.00822	1	3.22	0.00446	-10.473	0.4098
1	2.00	-0.0017	3	2.08	0.00324	3	1.87	0.01481	1	3.21	0.00447	-10.457	0.4130
0	-	-	7	2.03	0.01252	0	-	-	1	3.22	0.00435	-7.2414	0.5604
0	-	-	6	2.04	0.00903	1	2.28	0.00399	1	3.23	0.00465	-5.4420	0.5169
0	-	-	5	2.04	0.00725	2	2.28	0.01297	1	3.23	0.00475	-4.5598	0.4999
0	-	-	4	2.04	0.00590	3	2.24	0.0248	1	3.24	0.00485	-4.1628	0.4882

N: coordination number or occupancy; **R**: distance (Å); $\boldsymbol{\sigma^2}$: Debye-Waller factor (Å^2); $\mathbf{E_0}$: threshold energy shift (eV); **F**: fit error defined as $(\Sigma k^6(\chi_{exptl} - \chi_{calc})^2/\Sigma k^6\chi_{exptl}^2)^{1/2}$; Res: Resolution (Å). Unusually high and negative Debye-Waller factors are shown in blue and red, respectively. The best fits for each coordination number are shown in bold. Fit reported in the main manuscript is shown in green.

Table S3. Additional EXAFS (k=0.3-16 Å^{-1}) fitting results of samples containing the $Fe_2^{III/IV}$ intermediate (**X**) complex used for XAS.

		Fe-O/N			Fe-O/N			Fe-O			Fe-Fe					
N_{tot}*	S_0	N	R	σ^2	N	R	σ^2	N	R	σ^2	N	R	σ^2	E_0	F	Res.
2	0.9	1	2.12	-0.0003	1	2.00	-0.0005	0	-	-	0.65	2.78	0.0039	-9.0609	0.5662	0.099
											0.18	3.22	0.0043			
		1	2.11	-0.0002	1	1.99	0.0000	0.32	1.75	0.0021	0.65	2.77	0.0041	-10.909	0.5592	
											0.18	3.22	0.0043			
		1	2.21	-0.0003	1	2.00	-0.0003	0.65	2.10	-0.004	0.65	2.79	0.0045	-5.655	0.5077	
											0.18	3.22	0.0043			
		1	2.08	0.0058	1	2.00	0.00064	1.3	2.11	0.0032	0.65	2.78	0.0037	-7.6164	0.5225	
											0.18	3.22	0.0043			
3	0.9	2	2.09	0.0023	1	1.97	0.00039	0.65	1.77	0.0054	0.65	2.77	0.0041	-11.567	0.5140	0.099
											0.18	3.22	0.0043			
		1	**2.13**	**0.0009**	**2**	**2.00**	**0.00226**	**0.65**	**1.77**	**0.0048**	**0.65**	**2.77**	**0.0039**	**-11.602**	**0.5071**	
											0.18	**3.22**	**0.0043**			
		1	2.13	0.00029	2	2.00	0.0016	1.3	1.81	0.0135	0.65	2.77	0.0037	-12.799	0.5086	
											0.18	3.22	0.0043			
		1	2.12	0.00416	2	2.01	0.00412	0.32	1.74	0.0004	0.65	2.78	0.0040	-9.3145	0.4968	
											0.18	3.22	0.0043			
		1	2.16	0.00166	2	2.02	0.0025	0	-	-	0.65	2.78	0.0036	-8.2245	0.5360	
											0.18	3.22	0.0043			
4	0.9	**1**	**2.14**	**0.00455**	**3**	**2.01**	**0.00546**	**0.65**	**1.75**	**0.0028**	**0.65**	**2.78**	**0.0039**	**-10.874**	**0.4728**	0.099
											0.18	**3.22**	**0.0043**			
		2	2.11	0.0060	2	2.00	0.00434	0.65	1.75	0.0031	0.65	2.78	0.0039	-10.675	0.4780	
											0.18	3.22	0.0043			
		3	2.08	0.00571	1	1.98	0.00223	0.65	1.76	0.0034	0.65	2.78	0.0040	-10.686	0.4816	
											0.18	3.22	0.0043			
		1	2.15	0.00183	3	2.00	0.00376	1.3	1.77	0.0082	0.65	2.77	0.0037	-12.759	0.4824	
											0.18	3.22	0.0043			
		1	2.10	0.0120	3	2.03	0.00689	0.32	1.75	0.000	0.65	2.78	0.0040	-9.3722	0.4676	
											0.18	3.22	0.0043			
		1	2.21	0.0034	3	2.04	0.00486	0	-	-	0.65	2.79	0.0037	-7.2936	0.5373	

											0.18	3.22	0.0043			
5	0.9	4	2.03	0.00526	1	2.14	0.00344	0.65	1.75	0.0027	0.65	2.78	0.0040	-10.344	0.4583	0.099
											0.18	3.22	0.0043			
		3	**2.01**	**0.00432**	**2**	**2.11**	**0.00525**	**0.65**	**1.75**	**0.0028**	**0.65**	**2.78**	**0.0039**	**-10.188**	**0.4528**	
											0.18	**3.22**	**0.0043**			
		2	2.00	0.00403	3	2.08	0.00736	0.65	1.75	0.0028	0.65	2.78	0.0038	-10.075	0.4525	
											0.18	3.22	0.0043			
		1	2.01	0.00357	4	2.05	0.00990	0.65	1.75	0.0025	0.65	2.78	0.0039	-10.255	0.4542	
											0.18	3.22	0.0043			
		3	2.00	0.00254	2	2.10	0.00284	1.3	1.77	0.0070	0.65	2.78	0.0038	-12.300	0.4598	
											0.18	3.22	0.0043			
		3	2.03	0.00508	2	2.13	0.0079	0.32	1.75	0.0002	0.65	2.79	0.0040	-8.1549	0.4552	
											0.18	3.22	0.0043			
		3	2.04	0.00359	2	2.15	0.00545	0	-	-	0.65	2.79	0.0039	-7.2520	0.5333	
											0.18	3.22	0.0043			

*The reported total Fe-coordination number excludes the short Fe-O interaction(s) depicting the bridging ligand(s). **N**: coordination number or occupancy; **R**: distance (Å); $\boldsymbol{\sigma^2}$: Debye-Waller factor (Å^2); $\mathbf{E_0}$: threshold energy shift (eV); **F**: fit error defined as $(\Sigma k^6(\chi_{exptl} - \chi_{calc})^2/\Sigma k^6\chi_{exptl}^2)^{1/2}$; Res: Resolution (Å). Unusually high and negative Debye-Waller factors are shown in blue and red, respectively. The best fit for each coordination number is shown in bold. Fit reported in the main manuscript is shown in green.

Table S4. Additional EXAFS (k=0.3-16 Å^{-1}) fitting results of samples containing the $Fe_2^{III/IV}$ intermediate (**X**) complex used for XAS.

Scatterer type	**N**	**R (Å)**	**σ^2 (Å^2)**
Fe-O/N	3	2.02	0.0045
Fe-O/N	2	2.11	0.0065
Fe-O	0.65	1.75	0.0031
Fe-C	3	2.96	0.0046
Fe-Fe	0.65	2.79	0.0029
Fe-Fe	0.18	3.22	0.0043
E_0		-9.7563 eV	
F		0.37837	
Resolution		0.099 Å	

The best fit from **Table S3** was improved upon by the addition of a shell of Fe-C scattering interactions. **N**: coordination number or occupancy; **R**: distance; $\boldsymbol{\sigma^2}$: Debye-Waller factor; $\mathbf{E_0}$: threshold energy shift; **F**: fit error defined as $(\Sigma k^6(\chi_{exptl} - \chi_{calc})^2/\Sigma k^6\chi_{exptl}^2)^{1/2}$

Table S5. Additional EXAFS (k=0.3-16 Å^{-1}) fitting results of samples containing the $Fe_2^{III/IV}$ intermediate (**X**) complex used for XAS. Fe-carbon (Fe-C) interactions are included in the fit model.

Scatterer type	**N**	**R (Å)**	**σ^2 (Å^2)**
Fe-O/N	3	2.02	0.0045
Fe-O/N	2	2.12	0.0067
Fe-O	0.65	1.75	0.0033
Fe-C	1.61	2.97	0.0016
Fe-Fe	0.65	2.80	0.0036
Fe-Fe	0.18	3.22	0.0043
E_0		-9.5227 eV	
F		0.36566	
Resolution		0.099 Å	

The best fit from **Table S3** was improved upon by the addition of a shell of Fe-C scattering interactions. The occupancy of the Fe-C shell was treated as an adjustable parameter during the fit.

N: coordination number or occupancy; **R**: distance; σ^2: Debye-Waller factor; E_0: threshold energy shift; **F**: fit error defined as $(\Sigma k^6(\chi_{exptl} - \chi_{calc})^2/\Sigma k^6\chi_{exptl}^2)^{1/2}$

Table S6. Additional EXAFS (k=0.3-16 Å^{-1}) fitting results of samples containing the $Fe_2^{III/IV}$ intermediate (**X**) complex used for XAS. Fe-carbon (Fe-C) interactions are included in the fit model.

Scatterer type	N	R (Å)	σ^2 (Å^2)
Fe-O/N	3	2.02	0.0045
Fe-O/N	2	2.12	0.0067
Fe-O	0.65	1.75	0.0032
Fe-C	2	2.97	0.0025
Fe-Fe	0.65	2.80	0.0033
Fe-Fe	0.18	3.22	0.0043
E_0		-9.5711 eV	
F		0.36698	
Resolution		0.099 Å	

The best fit from **Table S3** was improved upon by the addition of a shell of Fe-C scattering interactions. The occupancy of the shell differs from that in **Tables S4** and **S5**.
N: coordination number or occupancy; **R**: distance; σ^2: Debye-Waller factor; E_0: threshold energy shift; **F**: fit error defined as $(\Sigma k^6(\chi_{exptl} - \chi_{calc})^2/\Sigma k^6\chi_{exptl}^2)^{1/2}$

Table S7. Additional EXAFS (k=0.3-16 Å^{-1}) fitting results of samples containing the $Fe_2^{III/IV}$ intermediate (**X**) complex used for XAS. Fe-carbon (Fe-C) interactions are included in the fit model.

Scatterer type	N	R (Å)	σ^2 (Å^2)
Fe-O/N	3	2.02	0.0044
Fe-O/N	2	2.12	0.0067
Fe-O	0.65	1.75	0.0033
Fe-C	2	2.97	0.0025
Fe-C	1	3.26	0.0099
Fe-Fe	0.65	2.80	0.0034
Fe-Fe	0.18	3.22	0.0043
E_0		-9.4284 eV	
F		0.36152	
Resolution		0.099 Å	

The best fit from **Table S3** was improved upon by the addition of two shells of Fe-C scattering interactions. The occupancies of the shells differ from those in **Table 1**.
N: coordination number or occupancy; **R**: distance; σ^2: Debye-Waller factor; E_0: threshold energy shift; **F**: fit error defined as $(\Sigma k^6(\chi_{exptl} - \chi_{calc})^2/\Sigma k^6\chi_{exptl}^2)^{1/2}$

Table S8. Fitting results of the second scan EXAFS (k=0.3-16 Å^{-1}) of samples containing the $Fe_2^{III/IV}$ intermediate (**X**) complex used for XAS. Fe-carbon (Fe-C) interactions are included in the fit model.

Scatterer type	N	R (Å)	σ^2 (Å^2)
Fe-O/N	5	2.07	0.0085
Fe-O	0.65	1.77	0.0040
Fe-C	3	2.96	0.0045
Fe-C	1	3.22	0.0054
Fe-Fe	0.65	2.80	0.0034
Fe-Fe	0.18	3.22	0.0043
E_0		-10.370 eV	
F		0.68898	
Resolution		0.099 Å	

N: coordination number or occupancy; **R**: distance; σ^2: Debye-Waller factor; E_0: threshold energy shift; **F**: fit error defined as $(\Sigma k^6(\chi_{exptl} - \chi_{calc})^2/\Sigma k^6\chi_{exptl}^2)^{1/2}$

Table S9. Distances and Mulliken Spin populations for the structural models of **X** discussed in the manuscript

Model	Distance (Å)						Mulliken Spin populations				
	Fe_1-Fe_2	Fe_1-O_1	Fe_1-O_2	Fe_2-O_1	Fe_2-O_2	Fe_1-O_t	Fe_1	Fe_2	O_1	O_2	O_t
$(\mu\text{-}O^{2-})_2$	2.809	1.955	1.965	1.759	1.750	2.030	4.248	-3.457	0.075	0.017	0.068
$\mu\text{-}[(O^{2-})\text{-}(OH^-)]$	2.971	2.028	2.029	1.691	1.943	2.003	4.308	-3.377	-0.149	0.029	0.090
$(\mu\text{-}O^{2-})_2$ + Y	2.831	1.935	1.971	1.768	1.759	2.053	4.237	-3.549	0.161	0.082	0.065
$\mu\text{-}[(O^{2-})\text{-}(OH^-)]$ + Y	2.983	2.010	2.032	1.697	1.967	2.019	4.304	-3.411	-0.078	0.031	0.087

Coordinates of the models from the table above:

$(\mu\text{-}O^{2-})_2$

Fe	-0.057278	0.097612	-0.006475
Fe	2.743711	-0.110872	0.052159
O	1.461830	0.175920	1.222093
C	-3.283465	0.627591	-2.983248
C	-2.236373	1.078998	-1.987219
O	-1.504187	0.138841	-1.449507
O	-2.116111	2.323531	-1.715430
C	0.715516	-4.205052	0.047881
C	0.990561	-2.717573	0.057922
O	-0.051393	-1.938076	-0.021847
O	2.198977	-2.306073	0.135177
C	-3.150160	-1.740292	0.934227
C	-2.659521	-0.674129	1.854849
N	-1.513577	0.094192	1.587376
C	-3.193452	-0.245531	3.050834
C	-1.369598	0.959750	2.598288
N	-2.369866	0.783830	3.502164
C	4.037719	0.913516	-2.974026
C	4.634090	-0.318295	-2.328923
O	5.585371	-0.944198	-2.876456
O	4.142702	-0.697655	-1.160824
C	4.361488	4.059450	0.292765
C	3.231657	3.048032	0.180092
O	2.026553	3.485380	0.184210
O	3.589320	1.809175	0.066299
C	6.340567	0.175212	0.806620
C	5.429430	-0.432687	1.820811
N	4.041343	-0.573060	1.636794
C	5.740949	-0.930528	3.067820
C	3.545092	-1.144152	2.740058
N	4.545478	-1.374411	3.629122
O	1.519553	0.108435	-1.179231
O	-0.151849	2.124884	0.009470
H	0.013810	-4.459079	0.849443
H	4.338501	1.796695	-2.400843

H	5.039528	3.771081	1.102268
H	-2.817506	0.018108	-3.764615
H	-4.026994	-0.001393	-2.479884
H	-3.783211	1.486148	-3.433946
H	0.243922	-4.485250	-0.900639
H	1.639887	-4.770612	0.172876
H	-4.010737	-2.259240	1.366233
H	-3.448793	-1.314980	-0.031114
H	-2.356853	-2.463501	0.725785
H	-4.061118	-0.570705	3.598543
H	-0.592838	1.698002	2.676965
H	-2.493706	1.312283	4.352785
H	4.384371	1.004519	-4.004772
H	2.947074	0.865943	-2.927567
H	4.946543	4.067921	-0.634891
H	3.969258	5.060674	0.478173
H	7.310259	0.407415	1.258422
H	6.502419	-0.499705	-0.040722
H	5.894654	1.088876	0.404651
H	6.680829	-0.998584	3.588110
H	2.506201	-1.360387	2.902541
H	4.435166	-1.792284	4.540078
H	0.723526	2.639395	0.064872
H	-0.850972	2.469394	-0.618500

μ-[(O^{2-})-(OH^{-})]

Fe	-0.184365	0.129519	-0.087865
Fe	2.777665	-0.064824	0.037070
O	1.477471	0.266373	1.066177
C	-3.305347	0.633157	-3.063610
C	-2.286166	1.107716	-2.059780
O	-1.577621	0.163882	-1.466870
O	-2.137836	2.345937	-1.814535
C	0.786635	-4.117286	0.004658
C	1.012717	-2.627925	-0.013902
O	-0.047169	-1.870639	-0.082948
O	2.209697	-2.171383	0.032960
C	-3.092454	-1.777475	1.006149
C	-2.567737	-0.707495	1.904086
N	-1.467015	0.104667	1.571618
C	-3.029404	-0.305464	3.137326
C	-1.283542	0.968517	2.582863
N	-2.209729	0.743869	3.545474
C	4.039856	0.915064	-3.130775
C	4.743312	-0.104975	-2.264180
O	5.891067	-0.525828	-2.541628
O	4.072527	-0.600004	-1.217904
C	4.319620	3.989648	0.483250

C	3.185945	3.016112	0.244195
O	1.983965	3.434884	0.288472
O	3.546902	1.785940	-0.011979
C	6.310051	0.131698	0.865903
C	5.353538	-0.442861	1.855384
N	3.965380	-0.554998	1.642075
C	5.617763	-0.933743	3.114901
C	3.424543	-1.093848	2.745291
N	4.399056	-1.338362	3.652314
O	1.417431	0.156609	-1.332861
O	-0.200046	2.132661	-0.062286
H	0.173712	-4.386665	0.871620
H	4.771035	1.461474	-3.728964
H	4.901846	3.670881	1.354825
H	-2.813605	0.036391	-3.839175
H	-4.038783	-0.014568	-2.570552
H	-3.816947	1.480863	-3.520593
H	0.234685	-4.417712	-0.892237
H	1.735701	-4.651930	0.046913
H	-3.944702	-2.280225	1.471161
H	-3.417316	-1.359138	0.046931
H	-2.318657	-2.518150	0.783771
H	-3.848124	-0.662535	3.737467
H	-0.529016	1.732702	2.623122
H	-2.295279	1.259455	4.409413
H	3.356081	0.398161	-3.816737
H	3.453447	1.604088	-2.522543
H	4.995546	3.990623	-0.378201
H	3.934395	4.996316	0.649551
H	7.290107	0.270802	1.331601
H	6.427658	-0.515332	-0.009302
H	5.948150	1.096906	0.499992
H	6.543258	-1.020649	3.657052
H	2.379247	-1.290560	2.895919
H	4.259995	-1.741860	4.567237
H	0.671985	2.643680	0.052677
H	-0.885424	2.516425	-0.681042
H	1.536090	-0.268020	-2.200249

$(\mu\text{-}O^{2-})_2$+ Y

Fe	0.167392	-0.086079	-0.346834
Fe	-2.659486	-0.235154	-0.302435
C	1.844580	-0.644982	-4.160754
C	1.699369	-1.142744	-2.744214
O	1.595785	-2.389216	-2.512647
O	1.668643	-0.229212	-1.785621

C	-0.541605	4.645778	-1.927886
C	-1.236401	4.051591	-0.687932
C	-1.259163	2.531010	-0.658552
O	-0.110823	1.912648	-0.649972
O	-2.400383	1.945832	-0.630968
C	2.936082	2.319190	0.681760
C	2.562877	1.185178	1.578398
N	1.549853	0.256931	1.278661
C	3.107968	0.847663	2.797536
C	1.497795	-0.611443	2.298542
N	2.423341	-0.281782	3.235655
C	9.577693	0.509710	-0.309213
C	8.125051	0.065003	-0.313134
C	7.707058	-1.118662	0.323761
C	7.144546	0.814474	-0.991428
C	6.373211	-1.538734	0.283562
C	5.805136	0.405070	-1.044159
C	5.413118	-0.779615	-0.402357
O	4.112362	-1.269917	-0.408609
C	-4.571191	-2.470559	-2.448831
C	-4.897612	-0.990800	-2.308407
O	-5.901046	-0.515050	-2.911740
O	-4.120066	-0.225932	-1.562232
C	-3.409179	-3.548295	2.152108
C	-2.577891	-3.069558	0.983670
O	-3.124218	-2.183043	0.217030
O	-1.384393	-3.523821	0.858386
C	-6.427937	0.611385	0.362560
C	-5.379719	0.727042	1.423592
N	-4.009277	0.413100	1.271053
C	-5.576332	1.146012	2.722315
C	-3.423786	0.643160	2.454426
N	-4.339458	1.085108	3.354428
O	-1.337086	-0.152771	0.868635
O	-1.387353	-0.488967	-1.490136
O	0.508069	-2.097734	-0.119529
H	1.999369	-1.477122	-4.849044
H	0.934470	-0.104551	-4.447194
H	-0.635838	5.737481	-1.922460
H	-0.996630	4.272465	-2.852457
H	-0.718536	4.395556	0.217612
H	-2.271458	4.399590	-0.632593
H	9.658430	1.594702	-0.172098
H	10.065378	0.273340	-1.265443
H	8.434305	-1.721948	0.860445
H	7.429759	1.735590	-1.493149
H	6.061328	-2.451172	0.780389
H	5.076135	1.003071	-1.582751
H	3.431096	-0.685470	-0.819202
H	-3.588613	-2.700602	-2.042662
H	-4.625954	-2.744472	-3.507816

H	-4.452677	-3.691983	1.862382
H	-3.002238	-4.459891	2.593030
H	-6.638918	-0.436666	0.119133
H	-6.113456	1.083376	-0.570809
H	-6.468352	1.472507	3.228869
H	-4.149286	1.334280	4.313439
H	-2.374133	0.500132	2.639440
H	3.051138	1.980878	-0.352817
H	2.163762	3.096312	0.671700
H	3.902757	1.296407	3.367819
H	0.837971	-1.457208	2.362128
H	-0.272908	-2.670660	0.191504
H	10.173819	0.029920	0.480049
H	3.883492	2.761219	1.013811
H	0.523143	4.399069	-1.943368
H	-5.321569	-3.077877	-1.917761
H	-3.372305	-2.740939	2.891825
H	-7.366213	1.077268	0.703836
H	0.993810	-2.461276	-0.911302
H	2.675988	0.058881	-4.233003
H	2.594651	-0.782082	4.095218

μ-[(O^{2-})-(OH^{-})]+ Y

Fe	0.232688	-0.000937	-0.422580
Fe	-2.741601	-0.179704	-0.278590
C	3.186052	-0.633970	-3.559270
C	2.235142	-1.067715	-2.477753
O	1.919890	-2.285467	-2.332249
O	1.769603	-0.104633	-1.685150
C	-0.540254	4.622325	-2.048632
C	-1.354138	4.035719	-0.882356
C	-1.325800	2.524178	-0.798610
O	-0.162127	1.933976	-0.764917
O	-2.444398	1.896936	-0.746253
C	2.884334	2.424690	0.709943
C	2.412085	1.340024	1.622339
N	1.416941	0.397482	1.284752
C	2.831967	1.069477	2.904863
C	1.258342	-0.409580	2.348887
N	2.095605	-0.025842	3.341307
C	9.610437	0.238310	-0.438152
C	8.146053	-0.113249	-0.288680
C	7.751996	-1.322563	0.316936
C	7.136119	0.743894	-0.755161
C	6.405593	-1.667960	0.443391
C	5.779431	0.409128	-0.639242
C	5.414931	-0.803779	-0.041268
O	4.088732	-1.214028	0.109908

C	-4.567902	-2.466234	-2.437745
C	-4.896298	-0.994049	-2.295386
O	-5.900871	-0.502537	-2.863525
O	-4.087252	-0.205590	-1.575623
C	-3.456192	-3.482669	2.087847
C	-2.609320	-2.952456	0.961897
O	-3.164869	-2.034984	0.212968
O	-1.413344	-3.368558	0.833578
C	-6.417666	0.629815	0.372047
C	-5.357854	0.862376	1.401108
N	-3.982876	0.560578	1.259142
C	-5.537843	1.393220	2.659548
C	-3.379723	0.906176	2.408807
N	-4.291371	1.409429	3.274395
O	-1.394843	-0.112452	0.751912
O	-1.336233	-0.478470	-1.622003
O	0.494146	-1.984858	-0.157167
H	4.034548	-0.097172	-3.123027
H	3.547010	-1.495417	-4.121441
H	-0.657496	5.710384	-2.070725
H	-0.882501	4.224419	-3.010170
H	-0.960273	4.419329	0.069192
H	-2.401133	4.343080	-0.950469
H	9.743120	1.296453	-0.685496
H	10.080291	-0.349289	-1.238401
H	8.511121	-2.003098	0.693995
H	7.406916	1.690304	-1.214670
H	6.107476	-2.600578	0.909723
H	5.021434	1.095340	-1.006260
H	3.434441	-0.565697	-0.225238
H	-3.584036	-2.696017	-2.035651
H	-4.617460	-2.731062	-3.498775
H	-4.505604	-3.555617	1.797260
H	-3.084478	-4.442310	2.449713
H	-6.587505	-0.440723	0.207108
H	-6.148421	1.056332	-0.596770
H	-6.427928	1.747712	3.150463
H	-4.094105	1.742720	4.206749
H	-2.328151	0.801906	2.606087
H	2.928324	2.078276	-0.326524
H	2.207280	3.287601	0.728601
H	3.577254	1.546289	3.517299
H	0.585363	-1.245610	2.404420
H	-0.285595	-2.551476	0.158989
H	10.173819	0.029920	0.480049
H	3.883492	2.761219	1.013811
H	0.523143	4.399069	-1.943368
H	-5.321569	-3.077877	-1.917761
H	-3.372305	-2.740939	2.891825
H	-7.366213	1.077268	0.703836
H	1.020716	-2.379668	-0.910112

H	2.675988	0.058881	-4.233003
H	2.185324	-0.476154	4.241299
H	-1.541827	-0.227494	-2.540919

REFERENCES:

(1) Bollinger, J. M., Jr.; Edmondson, D. E.; Huynh, B. H.; Filley, J.; Norton, J. R.; Stubbe, J. *Science* **1991**, *253*, 292-298.

(2) Parkin, S. E.; Chen, S.; Ley, B. A.; Mangravite, L.; Edmondson, D. E.; Huynh, B. H.; Bollinger, J. M., Jr. *Biochemistry* **1998**, *37*, 1124-1130.

(3) Dassama, L. M. K.; Yosca, T. H.; Conner, D. A.; Lee, M. H.; Blanc, B.; Streit, B. R.; Green, M. T.; DuBois, J. L.; Krebs, C.; Bollinger, J. M., Jr. *Biochemistry* **2012**, *51*, 1607-1616.

(4) Younker, J. M.; Krest, C. M.; Jiang, W.; Krebs, C.; Bollinger, J. M., Jr.; Green, M. T. *J. Am. Chem. Soc.* **2008**, *130*, 15022-15027.

(5) Price, J. C.; Barr, E. W.; Tirupati, B.; Bollinger, J. M., Jr.; Krebs, C. *Biochemistry* **2003**, *42*, 7497-7508.

(6) Münck, E. In *Physical Methods in Bioinorganic Chemistry*; Que, L., Jr., Ed.; University Science Books: Sausalito, CA, 2000, p 287-319.

(7) Sturgeon, B. E.; Burdi, D.; Chen, S.; Huynh, B. H.; Edmondson, D. E.; Stubbe, J.; Hoffman, B. M. *J. Am. Chem. Soc.* **1996**, *118*, 7551-7557.

(8) Ankudinov, A. L. PhD, University of Washington, 1996.

(9) Ankudinov, A. L.; Rehr, J. J. *Phys. Rev. B* **1997**, *56*, R1712.

(10) Frisch, M. J.; Trucks, G. W.; Schlegel, H. B.; Scuseria, G. E.; Robb, M. A.; Cheeseman, J. R.; Montgomery, J., J. A.; Vreven, T.; Kudin, K. N.; Burant, J. C.; Millam, J. M.; Iyengar, S. S.; Tomasi, J.; Barone, V.; Mennucci, B.; Cossi, M.; Scalmani, G.; Rega, N.; Petersson, G. A.; Nakatsuji, H.; Hada, M.; Ehara, M.; Toyota, K.; Fukuda, R.; Hasegawa, J.; Ishida, M.; Nakajima, T.; Honda, Y.; Kitao, O.; Nakai, H.; Klene, M.; Li, X.; Knox, J. E.; Hratchian, H. P.; Cross, J. B.; Bakken, V.; Adamo, C.; Jaramillo, J.; Gomperts, R.; Stratmann, R. E.; Yazyev, O.; Austin, A. J.; Cammi, R.; Pomelli, C.; Ochterski, J. W.; Ayala, P. Y.; Morokuma, K.; Voth, G. A.; Salvador, P.; Dannenberg, J. J.; Zakrzewski, V. G.; Dapprich, S.; Daniels, A. D.; Strain, M. C.; Farkas, O.; Malick, D. K.; Rabuck, A. D.; Raghavachari, K.; Foresman, J. B.; Ortiz, J. V.; Cui, Q.; Baboul, A. G.; Clifford, S.; Cioslowski, J.; Stefanov, B. B.; Liu, G.; Liashenko, A.; Piskorz, P.; Komaromi, I.; Martin, R. L.; Fox, D. J.; Keith, T.; Al-Laham, M. A.; Peng, C. Y.; Nanayakkara, A.; Challacombe, M.; Gill, P. M. W.; Johnson, B.; Chen, W.; Wong, M. W.; Gonzalez, C.; Pople, J. A.; Inc., G., Ed.; Gaussian Inc.: Wallingford, CT, 2003.

(11) Nordlund, P.; Eklund, H. *J. Mol. Biol.* **1993**, *232*, 123-164.

(12) Becke, A. D. *Phys. Rev. A* **1988**, *38*, 3098-3100.

(13) Pedew, J. P.; Wang, Y. *Phys. Rev. B* **1988**, *38*, 12228-12232.

(14) Schäfer, A.; Horn, H.; Ahlrichs, R. *J. Chem. Phys.* **1992**, *97*, 2571-2577.

(15) Han, W.-G.; Liu, T.; Lovell, T.; Noodleman, L. *J. Am. Chem. Soc.* **2005**, *127*, 15778-15790.

(16) Becke, A. D. *J. Chem. Phys.* **1993**, *98*, 5648-5652.

(17) Lee, C. T.; Yang, W. T.; Parr, R. G. *Phys. Rev. B* **1998**, *37*, 785-789.

(18) Klamt, A.; Schuurmann, G. *J. Chem. Soc. Perkin Trans* **1993**, *2*, 799-805.

(19) Barone, V.; Cossi, M. *J. Phys. Chem. A* **1998**, *102*, 1995-2001.

(20) Riggs-Gelasco, P. J.; Shu, L.; Chen, S.; Burdi, D.; Huynh, B. H.; Que, L., Jr.; Stubbe, J. *J. Am. Chem. Soc.* **1998**, *120*, 849-860.